

Structural defects in chromium-ion-implanted vitreous silica

Hideo Hosono* and Robert A. Weeks

Department of Materials Science and Engineering, Vanderbilt University, Nashville, Tennessee 37235

(Received 2 June 1989; revised manuscript received 26 July 1989)

Structural defects and their concentrations have been determined in high-purity vitreous silica implanted with 0.5×10^{16} to 6×10^{16} Cr ions/cm². Electron paramagnetic resonance (EPR) and optical-absorption spectra have been measured at 9.7 GHz and from 5 to 8 eV, respectively. A band with a peak around 7.5 eV increases with increasing dose and is attributed to a Si—Si bond similar to that in a Si₂H₆ molecule. This band has been called the Si—Si homobond. The concentrations of the homobonds and implanted Cr ions are of the same order of magnitude in the implanted layers at each dose level. A component of the EPR spectra is attributed to an *E'*-type paramagnetic state in which one of the Si bonds is to another Si, i.e., the Si—Si homobond. Another paramagnetic defect is the peroxy radical. The concentration of the *E'*-type center is high near the surface and decreases monotonically with depth. On the other hand, beginning at the surface the concentration of the peroxy radical increases to a maximum near the peak of the Cr-ion distribution and then decreases at greater depths. These complementary profiles suggest that oxygens are displaced in the direction of the ion beams and that these two defects are a paramagnetic Frenkel pair.

I. INTRODUCTION

Ion implantation is a processing technique that can modify the surface and near-surface region of materials.¹ A number of papers have been devoted to effects of ion implantation into glasses.² In case of vitreous (*v*-) silica, it has been reported that implantation of inert gas ions such as He⁺ and Ar⁺ alters the refractive index via radiation-induced density change and produces a group of optical-absorption bands which are due to alternation of the structure.² Further, the formation kinetics of the *E'* center³ has been discussed.⁴

We consider that implantation of transition-metal ions into *v*-SiO₂ is effective in modifying the optical and magnetic properties because these ions may react chemically with oxygens in the substrate structure. Interactions of implanted transition-metal ions with substrate structures have not been extensively investigated. For instance, Antonini *et al.*⁵ reported that implantation of 47.5-MeV Ni ions appears to produce optical bands due primarily to intrinsic structural defects in vitreous silica. Stark *et al.*⁶ shows that absorption bands in the range of 1–6 eV produced by implantation of Cr, Mn, or Fe into *v*-SiO₂ are due primarily to structural modifications of the Si-O network. Peaks at 5 and 5.8 eV in one band are attributed to the neutral oxygen vacancy⁷ and *E'* center,⁸ respectively. Knowledge of the types of structural defects produced and their concentrations as a function of dose and depth is needed to consider the interaction between substrate and implanted ion.

Here we report structural defects produced in vitreous SiO₂ by implantation of chromium ions. The EPR spectra of the Cr-implanted samples are primarily due to structural defects, since components due to Cr have intensities more than an order of magnitude less intense than those due to structural defects. Thus the EPR spectra can provide data on the dose and depth dependence of

these defects without severe interference from ion specific paramagnetic states. Three types of paramagnetic structural defects have been identified and their dose and depth dependence have been measured by electron paramagnetic resonance spectroscopy. Information about two types of diamagnetic defects has been obtained from vacuum ultraviolet (vuv) and ultraviolet absorption spectra.

II. EXPERIMENTAL DETAILS

Type-III (Ref. 9) *v*-SiO₂ (spectrosil 1, impurities; 200 wt. ppm OH, 50 ppm Cl) was chosen because some type-IV *v*-SiO₂ gives an intense absorption band in the vuv region in the as-delivered state.^{10,11} Glass plates, 2.0 cm diam \times 0.1 cm thick, were used as substrates. Chromium +1 ions were implanted into the substrates at room temperature to doses of 0.5×10^{16} , 1×10^{16} , 3×10^{16} , and 6×10^{16} ions/cm². The acceleration voltage and dose rate were 160 keV and $2.5 \mu\text{A}/\text{cm}^2$, respectively. The nominal implantation dose was determined by charge integration. Implantation depth profiles determined by Rutherford backscattering (RBS) technique (⁴He⁺ 2 MeV) using a TRIM calculation program¹² were Gaussian in shape with the peak concentration at a depth of 0.14 μm and full width of half maximum (FWHM) of approximately 0.14 μm for all the samples.

Vacuum uv absorption measurements were made over the wavelength of 250–150 nm using a single beam spectrophotometer (JASCO model monochromator, 0.25 m; light source, D₂-discharge lamp). The spectrum for the substrate before implantation was subtracted from that for the substrate after implantation in order to compensate the surface reflection losses and absorptions due to the substrate. Ultraviolet (uv) absorption spectra over the wavelength of 200–350 nm were measured with a double beam spectrophotometer (Cary model 14). An unimplanted substrate was placed in the reference beam

so as to cancel surface reflection losses.

X-band EPR spectra were measured with a homodyne-type spectrometer (Bruker ER 200 D) at 110 or 300 K applying 100 kHz field modulation. Microwave power in the cavity is ≈ 200 mW at an attenuation of 0 dB. Since signals are weak under measurement conditions appropriate for observing the unsaturated and undistorted shapes, accumulation was made over 40–300 scans to improve the signal-to-noise ratio. The g value and concentration, respectively, were determined with a strong pitch standard sample (Bruker, $g = 2.0028$) and a recrystallized $\text{CuSO}_4 \cdot 5\text{H}_2\text{O}$ crystal using a comparison method.

Chemical etching technique was applied to measure the depth concentrations of paramagnetic structural defects produced in the implanted layers. Samples implanted with Cr^+ to doses of 0.5×10^{16} and 6×10^{16} ions/cm² were employed. Approximately 1 wt. % HF aqueous solution (one part of 45 wt. % HF was mixed with 100 parts of distilled water) was used as an etchant. Two pieces ($5 \times 3 \times 1$ mm³) of the samples were used for each series of experiments. After these pieces were immersed in the fresh etchant at 20°C for a desired time, they were washed with distilled water, dried with air jet, and one piece each was used for EPR and RBS measurement. These procedures were repeated until most of the implanted layers were removed.

III. RESULTS

A. Vuv-uv absorption

Figure 1 shows vuv and uv absorption spectra of the implanted samples. No absorptions are resolved in the region of the tail of the absorption edge for the unimplanted substrates. Since the substrate is $\nu\text{-SiO}_2$, prepared by flame hydrolysis of SiCl_4 (type III), this result is consistent with the data in Ref. 11. In Ref. 11 correlations between vuv absorptions and preparation

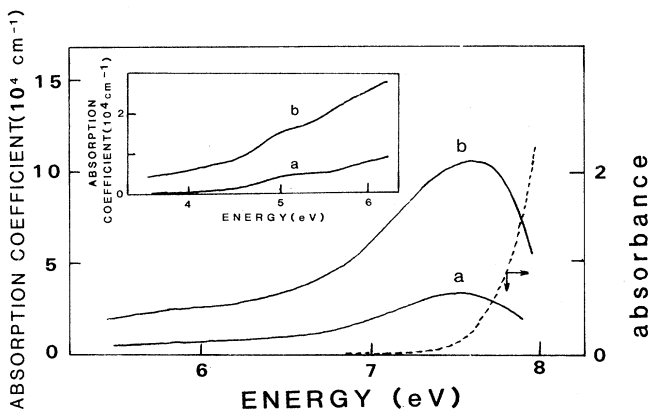


FIG. 1. Vacuum uv and uv absorptions induced by ion implantation. (a) Cr 0.5×10^{16} ions/cm², (b) Cr 3×10^{16} ions/cm². The absorption coefficients were calculated by assuming the thickness of implanted layers to the $0.14 \mu\text{m}$, which corresponds to FWHM of the backscattering spectra. The dashed trace is the absorption spectrum of unimplanted substrate.

processes of $\nu\text{-SiO}_2$ are reported. An intense absorption and a weak but distinct absorption are resolved around 7.5 and 5 eV, respectively. Intensities of both bands increased with dose.

B. EPR spectra

No EPR signals were detected for the substrates before implantation under operation conditions described below. Figure 2 shows EPR spectra of the substrates after implantation. Four types of signals are noted; a signal having a characteristic shoulder at $g = 2.067$ is assigned to a peroxy radical (POR) on the basis of the g values at the three fields indicated by small arrows in 2(a). These values agree well with those of POR in $\nu\text{-SiO}_2$ (type IV, suprasil W1) irradiated by ionizing rays.¹³ Nonbridging oxygen hole centers (NBOHC), which give a signal characterized by different g values (2.0010, 2.0095, 2.078),¹³ have not been resolved in the spectra reported here.

Based on the close similarity of g values, of line shape in neutron-irradiated $\nu\text{-SiO}_2$,¹⁴ and of saturation behavior (easily saturable, > 40 dB at 300 K, > 50 dB at 110 K), one component is assigned to an E' center.³ The E' center induced by implantation has an anisotropic line shape, that due to orthorhombic symmetry, $g = 2.0018, 2.0014, 2.0005$, linewidth (spacing between two extremes) of ≈ 0.3 mT, and begins to be saturated at a power level of approximately 50 dB at 110 K.

In addition to the POR and E' -center components, an absorption with a slightly asymmetric shape is dominant

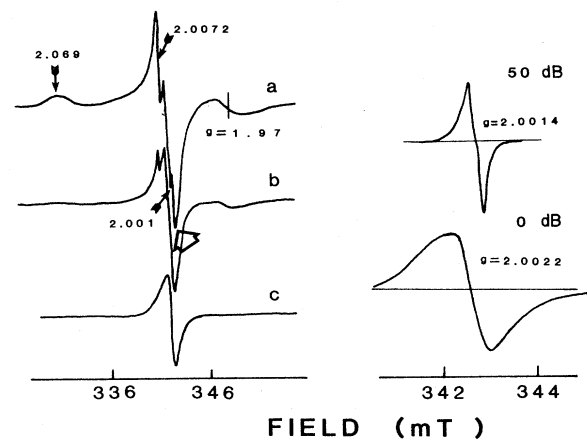


FIG. 2. EPR spectra of Cr-implanted substrates. Changes with dose (left). a, 0.5×10^{16} ions/cm²; b, 3×10^{16} ions/cm²; c, 6×10^{16} ions/cm². These spectra were obtained at 110 K and an attenuation of 0 dB with the same spectrometer sensitivity. Small arrows indicate magnetic fields used for determination of g values of POR. The component due to X signal is indicated by big arrows. Changes with microwave power (right). Sample; Cr 6×10^{16} ions/cm² implanted substrate. Top 50 dB; bottom, 0 dB. Measurement conditions: Temp., 110 K; modulation amplitude, 0.05 mT. The spectrometer sensitivity for measuring the top signal is 30 times greater than that for the bottom signal.

in the spectrum of samples implanted to a dose of 6×10^{16} ions/cm² measured at a power level of 0 dB (at 110 K). This signal, which will be temporarily called *X* signal, is seen in the spectra of the other samples as indicated by a big arrow. The *X* signal can be discriminated easily from *E'*-center signals produced by implantation.^{15,16} The *X* center has a line shape that is almost isotropic, a *g* value equal to 2.0022, linewidth of 0.8 mT, and does not saturate appreciably up to the 0-dB power level at 110 K.

Since POR and *X* signals coexist and overlap closely in the central part of the spectrum of the sample except for the highest implanted dose, the relative intensities of the respective signals were evaluated as follows; almost "pure" line shapes of the POR signal and *X* signal are seen in the spectra of Cu-implanted (1×10^{16} ions/cm²) samples measured at 110 K with 0 dB and the samples implanted with Cr⁺ to a dose of 6×10^{16} Cr ions/cm², respectively. By using these two "pure" shapes, a ratio of amplitude of the two signals was found which reproduced the observed shape. The concentration evaluation of POR and *X* center from spectra on which both of these two signals appear was made using this procedure.

The concentrations of the EPR composites are plotted in Fig. 3 as a function of dose. For the calculation of defect concentrations, the thicknesses of the implanted layers were assumed to be equal to the FWHM of the distribution of the implanted Cr ions, all evaluated from RBS spectra, i.e., 0.14 μ m. It is obvious from the figure that the POR concentration decreases monotonically with dose and almost disappears in the sample implanted with 6×10^{16} ions/cm².

An absorption with linewidth of ≈ 3 mT was seen near $g = 1.97$, and its intensity decreases monotonically with dose and is not detected in the sample implanted to a dose of 6×10^{16} ions/cm². This signal is not seen in *v*-

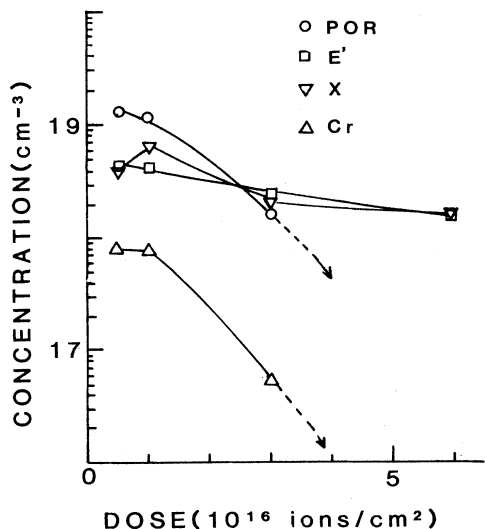


FIG. 3. Dose dependence of concentrations of paramagnetic centers. The thicknesses of implanted layers were assumed to be 0.14 μ m. The concentrations of EPR active Cr ions in the figure are values in the case that a signal centered at $g = 1.97$ is assumed to be responsible for an isolated paramagnetic state with $S = \frac{1}{2}$.

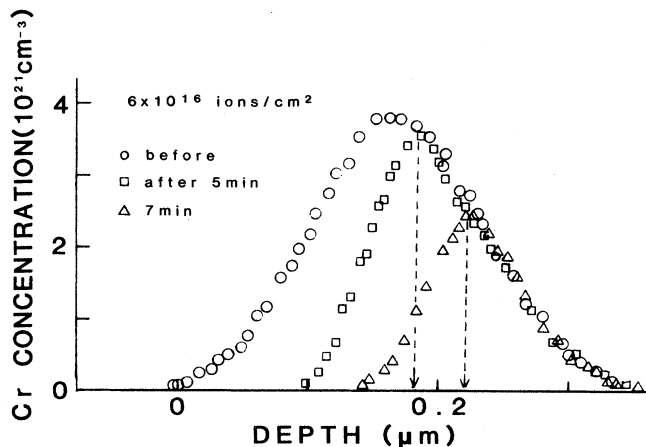


FIG. 4. Changes in depth profiles of Cr ions implanted into *v*-SiO₂ with etching. Arrows indicate the surface positions after etching scaled from that before etching.

SiO₂ implanted with other first transition series metal ions.¹⁵ Therefore we assume that this signal is not due to intrinsic structural defect but to paramagnetic states of implanted chromium ions.^{17,18} No discussion about this signal is given in this report.

C. Depth concentration of paramagnetic centers

Figure 4 shows the changes in depth profiles of Cr ions with etching. The profile for the sample before etching is almost Gaussian in shape with peak concentration at a depth of approximately 0.14 μ m from the surface and FWHM of approximately 0.14 μ m. The thickness of materials removed by etching can be determined by comparing the spectrum after etching with that before etching. This comparison gives the thickness removed with a precision of ± 0.005 μ m.

Figure 5 shows changes in EPR spectra with etching

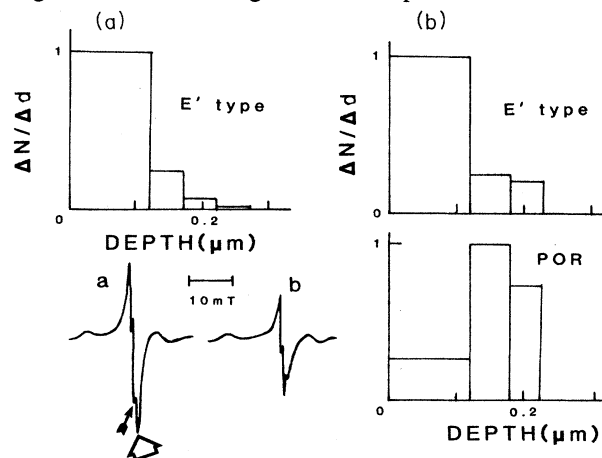


FIG. 5. Depth concentrations of *E'*-type center and peroxy radical (POR). *DN*, number of centers removed; *Dd*; thickness removed by etching. (a) Sample; implanted to dose of 6×10^{16} ions/cm². (b) 0.5×10^{16} ions/cm². Examples of changes in EPR spectra with etching (left bottom). Sample; 0.5×10^{16} ions/cm². *a* before; *b*, after 4-min etching. Spectrometer sensitivity is kept constant. Small and large arrows indicate POR and *E'*-type signals, respectively.

and the depth concentrations of the X center and POR evaluated from the experiment. It is obvious that the intensity of X signal relative to that of POR decreases markedly with etching time. Depth profiles of these two center are quite different in the sample implanted to a dose of 0.5×10^{16} ions/cm²; the concentration of X centers is highest near the surface and decreases monotonically with depth. On the other hand, the depth dependence of POR is not monotonic. The highest concentration is in the region of the peak of the distribution of the implanted Cr ions. In the sample (in which no significant contribution of POR to the spectrum is seen) implanted to a dose of 6×10^{16} ions/cm², a similar profile was obtained for the X center.

IV. DISCUSSION

Only peroxy radicals were observed in the present samples as oxygen-related paramagnetic defects. The major oxygen-related EPR center in type-III SiO₂ irradiated by ionizing rays such as gamma rays is not POR but NBOHC.^{13,19} Thus it is clear from this sharp contrast that displacement processes play an essential role in the formation of defects by Cr-ion implantation. We will discuss properties and concentrations of intrinsic structural defects, especially oxygen-deficient-type defects, and interactions of implanted ions with substrates from a view of the formation of structural defects.

A. Defects responsible for the 7.5- and 5-eV bands

First, we will consider the 7.5-eV optical band. Two structural models have been proposed for this band; one is the POR,^{13,20} which is paramagnetic and is due to an oxygen-excess-type defect. Another is the Si—Si homobond,¹⁶ which is diamagnetic and an oxygen-deficient-type defect. The dose dependence of POR shown in Fig. 3 is the reverse of that of the 7.5-eV band. Therefore POR cannot be a major part of the 7.5-eV band. Let us suppose that the absorptivity at the apparent peak of the band around 7.5 eV is completely controlled by the absorption of Si—Si homobond and POR. Then, the concentration of the homobond can be estimated from the absorption cross-section data ($\sigma_{\text{Si-Si}} = 8 \times 10^{-17}$ cm²,²¹ $\sigma_{\text{POR}} = 1.3 \times 10^{-16}$ cm²) of these two defects reported in Refs. 22 and 20, and the POR concentration obtained here (Fig. 3). The absorptivity estimated from the number of POR and its absorption cross section was at most no more than 10% of that of the observed band. The estimated homobond concentrations are plotted in Fig. 6 as a function of dose together with the concentrations of implanted Cr ions and E' and X centers.

The concentrations of Si—Si homobond increase from 4×10^{20} to 2×10^{21} cm⁻³, being comparable to the mean concentrations of Cr ions in the implanted layers at each dose level. According to this estimation, the fraction of Si atoms forming the homobond increases from 4 to 16% of the total Si atoms in the implanted layers on the assumption that the homobonds are randomly distributed in the implanted layers.

The defect giving the 5-eV band (so-called B_2 center) is

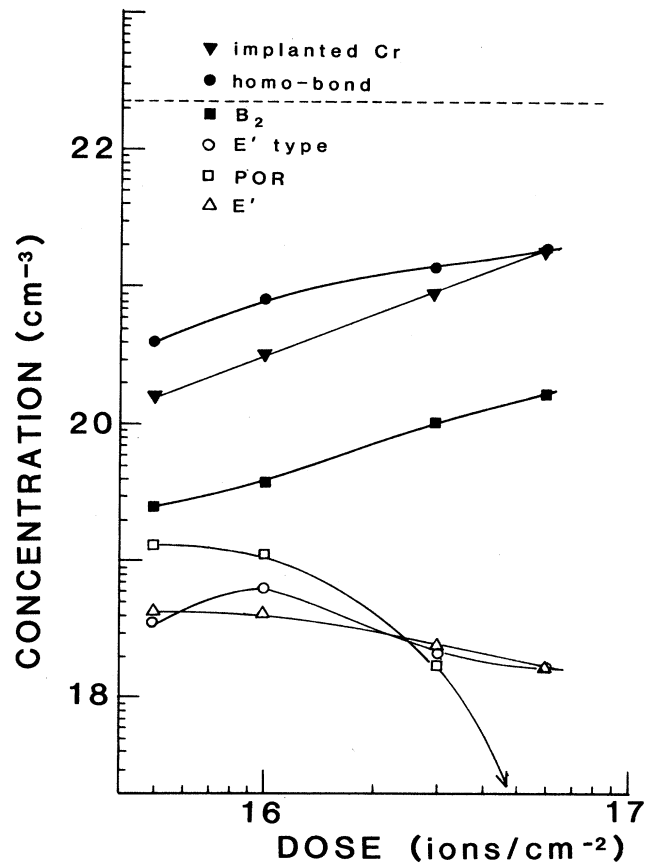


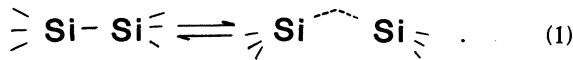
FIG. 6. Dose dependence of concentrations of intrinsic structural defects produced by ion implantation. The thickness of implanted layers was assumed to be $0.14 \mu\text{m}$, which corresponds to FWHM of the RBS spectra. The dashed line indicates the concentration of Si atoms in the substrate.

well resolved in ion-bombarded ν -SiO₂ and has been assigned to a neutral oxygen vacancy.⁷ The concentrations of B_2 centers can be evaluated from the absorptivity in the deconvoluted spectrum reported in Ref. 6 by using an absorption cross section (2×10^{-17} cm²) reported in Ref. 22. The evaluated concentration plotted in Fig. 6 increases monotonically with dose and is about an order of magnitude less than the homobond concentration.

B. Estimation of fictive temperature in implanted layers

Energetic ions dissipate their energies in a very short time. We suppose that in the implanted layers a structure is produced corresponding to equilibrium structure at temperatures far higher than the fictive temperature T_f (≈ 1300 K) of the substrate before implantation.

Here, we will make an estimation of the T_f of the implanted layers. A thermal equilibrium is assumed between the configurations of the Si—Si homobond and neutral oxygen vacancy (B_2 center) as in Ref. 22.



O'Reilly and Robertson²³ calculated the energy of various point defects including the two above. They reported that the homobond configuration is more stable than the oxygen vacancy configuration. Thus the B_2 center and the homobond may be regarded as unrelaxed oxygen vacancy and relaxed oxygen vacancy, respectively. Imai *et al.*²² experimentally obtained 1 eV as the enthalpy difference between these two defects by using ν -SiO₂ prepared by the chemical-vapor-deposition-(CVD-) soot remelting process.²⁴ According to these reports, the equilibrium constant K should increase with increasing T_f . The value of K evaluated from Fig. 6 is $\approx 10^{-1}$ over the dose range examined, which is about 3 orders of magnitude greater than that (5×10^{-4}) in ν -SiO₂ with $T_f = 1300$ – 1600 K. Provided that this enthalpy difference remains unchanged, the T_f in the ion-implanted ν -SiO₂ layers is estimated to be ≈ 5000 K. This value is comparable to the T_f (≈ 4000 K) in neutron-irradiated ν -SiO₂ reported by Geissberger and Galeener.²⁵ They evaluated the T_f from the intensities of T_f -sensitive specific Raman bands.²⁶ It is of interest that two different approaches lead to a comparable T_f in particle-bombarded ν -SiO₂. We suppose that realization of a state corresponding to extremely high temperatures is associated closely with the "thermal spike" model of particle irradiation damage.²⁷ Local heating due to energy generated in the collision of energetic ions with the substrate melts a microscopic volume around the sites of the primary knocked-on atoms and these extremely small volumes are rapidly quenched.

C. Defect structure of X center

No EPR signal similar to the X signal has been reported in ν -SiO₂ irradiated by ionizing rays, to our knowledge. A report examining paramagnetic defects in nonstoichiometric amorphous SiO_x provides a basis for proposing a model for the X center. Holzenkämpfer *et al.*²⁸ measured EPR spectra in as-deposited and He⁺-bombarded α -SiO_x films over a wide range of x ($0 \leq x \leq 2$), reporting the variation in the g values and linewidths of E' -type centers as a function of x . They reported that EPR components with g value 2.0022 and linewidth 0.8 mT are observed in $x \approx 1.6$ components. These values correspond to the X center in all implanted samples. The less-saturable nature of the paramagnetic states in these oxygen-deficient materials is consistent with that of the X center. Based on these similarities, the X center is identical with the E' -type center in heavily oxygen-deficient ν -SiO₂. This E' -type center is assumed to have a structure which is obtained by replacing one of the three oxygens in the standard E' center by a silicon ion. If the dangling bond is replaced by an oxygen, this structure corresponds to that with $x = 1.5$.

The appearance of the paramagnetic defect characteristic of oxygen-deficient silica is quite compatible with the production of the Si—Si homobond in concentrations from 3 to 16 % of the total Si atoms. Here, let us evalu-

ate the degree of off stoichiometry in the implanted layers from the homobond concentration: Oxygens are assumed to combine preferably with silicons. Under this constraint, the relation between stoichiometry (SiO_x) and the number of Si—O bonds ($N_{\text{Si-O}}$) or Si—Si bonds ($N_{\text{Si-Si}}$) is given by Eq. (2) or (3);

$$N_{\text{Si-O}} = 2x, \quad (2)$$

$$N_{\text{Si-Si}} = 2 - x. \quad (3)$$

Equation (3) gives the relation between x and $N_{\text{Si-Si}}$ per cm³ ($C_{\text{Si-Si}}$):

$$C_{\text{Si-Si}} = (6.03 \times 10^{23}) d \frac{2-x}{28+16x}, \quad (4)$$

where d is the density of the implanted layers. Here, the density (2.2 g/cm³) of the unimplanted ν -SiO₂ is used as the value of d . Then, Eq. (4) is obtained;

$$C_{\text{Si-Si}} = (1.33 \times 10^{24}) \frac{2-x}{28+16x}. \quad (5)$$

Putting $C_{\text{Si-Si}}$ estimated (Fig. 6) into Eq. (5), we get the following stoichiometry x for the samples implanted with each dose: SiO_{1.98} (0.5×10^{16} ions/cm²), SiO_{1.96} (1×10^{16}), SiO_{1.94} (3×10^{16}), and SiO_{1.92} (6×10^{16}). The fraction of oxygen-deficiencies is much less than that ($x \approx 1.6$) estimated from the paramagnetic properties of the X center already observable in the sample implanted with 0.5×10^{16} ions/cm². We suggest that this result may be explained if the homobonds are not distributed randomly in the implanted layers.

D. Interaction of implanted Cr ions with substrate

The number of Si—Si homobonds in the implanted layer increases monotonically with increasing dose and is comparable to the number of chromium ions implanted as shown in Fig. 6. This equivalence is attributed, tentatively, to chemical interactions of implanted Cr ions with the substrates: a major fraction of chromium ions is deposited as cations. The implanted ions, therefore, attract oxygens as ligands so as to reserve local electroneutrality. If the chemical interaction of an implanted ion with oxygens is strong, the implanted ion reacts with some of the oxygens displaced from the glass network to form oxides, leaving Si—Si homobonds and neutral oxygen vacancies. Formation of these oxygen-deficient-type defects is specific to implanted ion species and is related closely to the chemical state of ions in implanted layers.¹⁵

The concentration of POR, which is an oxygen-excess-type defect and produced as a consequence of displacement of oxygen by collision, decreases monotonically with dose as shown in Fig. 6. This trend is consistent with this hypothesis, since the number of oxygens needed for the oxide formation increases with dose, the remaining POR concentration decreases as a consequence of reaction of implanted Cr ions with displaced oxygen ions. Therefore fewer oxygen ions form POR as the dose increases.

E. Depth concentrations of paramagnetic defects

It is obvious from Fig. 5 that the X -center (E' -type defect associated with Si—Si homobond) concentration is highest near the surface region while the POR maximum concentration is in the deeper region where the peak of the implanted Cr distribution is present. This result is interpreted as follows. Chromium ions displace oxygens via collision, leaving oxygen-deficient defects such as Si—Si homobonds in the near-surface region. These displaced oxygens combine with the implanted ions and deposit as the oxides or react with Si—O—Si bonds to form POR and/or peroxy linkages. Therefore X center and POR may be regarded as a pair of Frenkel-type paramagnetic defects associated with oxygen.

V. CONCLUSION

1. Silicon—silicon homobonds are produced by ion implantation of Cr. Their concentration increases with increasing dose and is of the same order of magnitude as that of the implanted Cr ions at each dose.

2. E' , E' -type, B_2 , and POR centers are also produced in the concentrations that are more than an order of mag-

nitude less than the concentrations of the homobonds.

3. The E' -type center is assigned to localization of an electron in a Si ion which is bonded to two oxygens and one Si, i.e., the Si—Si homobond.

4. The depth concentration profiles of the E' -type center associated with the homobond and POR are complementary in the region from the surface to near the center of the implanted layer. This result suggests that oxygens are displaced in the direction of the ion beam and these two defects are a paramagnetic Frenkel pair.

5. Based on the ratio of concentration of B_2 center to the homobond, the implanted layers have a high fictive temperature.

ACKNOWLEDGMENTS

The authors thank Prof. H. Imagawa of Toyo University, Japan, for vuv measurements and Dr. R. Zuhr of Oak Ridge National Laboratory for RBS measurements. The stay of H. H. at Vanderbilt University was supported by the Japanese Ministry of Education, Science and Culture. This research was supported in part by a NSF Grant No. DMR-8513731.

*On leave from Department of Materials Science and Engineering, Nagoya Institute of Technology, Showa-ku, Nagoya 466, Japan.

¹P. D. Townsend, Rep. Prog. Phys. **50**, 501 (1987).

²P. Mazzoldi and G. W. Arnold, in *Ion Beam Modification of Insulators*, edited by P. Mazzoldi and G. W. Arnold (Elsevier, Amsterdam, 1987), Chap. 5.

³R. A. Weeks, J. Appl. Phys. **27**, 1376 (1956).

⁴R. A. B. Devine and A. Golanski, J. Appl. Phys. **54**, 3833 (1983).

⁵M. Antonini, P. Camagri, P. N. Bibson, and A. Manari, Radiat. Eff. **65**, 41 (1982); J. Non-Cryst. Solids **44**, 321 (1981).

⁶J. D. Stark, R. A. Weeks, G. Whichard, D. L. Kinser, and R. A. Zuhr, J. Non-Cryst. Solids **95-96**, 685 (1987).

⁷G. W. Arnold, IEEE Trans. Nucl. Sci. **NS-20**, 220 (1973).

⁸R. A. Weeks and C. M. Nelson, J. Appl. Phys. **31**, 1555 (1960).

⁹R. Bruckner, J. Non-Cryst. Solids **5**, 123 (1970).

¹⁰I. P. Kaminow, B. G. Bagley, and C. G. Olson, Appl. Phys. Lett. **32**, 98 (1978).

¹¹H. Imai, K. Arai, T. Saito, S. Ichimura, H. Nonaka, J. P. Vigouroux, H. Imagawa, H. Hosono, and Y. Abe, in *The Physics and Technology of Amorphous SiO₂*, edited by R. A. B. Devine (Plenum, New York, 1988), p. 153.

¹²J. F. Ziegler, J. P. Biersack, and U. Littmark, *The Stopping and Range of Ions in Solids* (Pergamon, New York, 1985).

¹³M. Stapelbroek, D. L. Griscom, E. J. Friebele, and G. H. Sigel, Jr., J. Non-Cryst. Solids **32**, 313 (1979).

¹⁴R. A. Weeks, in *Interaction of Radiation with Solids*, edited by A. Bishay (Plenum, New York, 1967), p. 55.

¹⁵H. Hosono, R. A. Weeks, H. Imagawa, and R. Zuhr, J. Non-Cryst. Solids (to be published).

¹⁶A possibility that the shape of the X signal might be a strongly saturated E' resonance is denied on the basis of the following experimental results. In Cu-implanted ν -SiO₂ (0.3×10^{16} – 6×10^{16} ions/cm²) (Ref. 15), the concentrations of E' center and POR are comparable to those in ν -SiO₂ im-

planted with Cr ions to a dose of 0.5×10^{16} ions/cm². If the X signal is a strongly saturated E' resonance, the X signal should appear to a comparable extent at 110 K and 0 dB. But only POR is observable in the spectrum. At 300 K, E' center in Cu-implanted samples begins to be saturated at a level > 40 dB and its intensity at 0 dB is about $\frac{1}{300}$ of that in the saturation-free case. No significant changes in the linewidth or shape were noted with increasing power. On the other hand, X center and POR show no serious power saturation even at 110 K up to 0 dB. The absorption area of the signal (X resonance, in the sample implanted with Cr⁺ to a dose of 6×10^{16} ions/cm²) measured at 110 K and 0 dB is greater than that of the signal (E' resonance) at 110 K and 50 dB by a factor of about 300, which is close to the ratio of square root of power [$(10^3)^{1/2} = 320$]. This result indicates that the contribution of E' center to the signal (X signal) measured at 0 dB is extremely small. Therefore the X signal is not a strongly saturated shape of E' resonance but due to a different paramagnetic species.

¹⁷J. T. Fournier, R. T. Landry, and R. H. Bartram, J. Chem. Phys. **55**, 2522 (1971).

¹⁸D. L. Griscom, J. Non-Cryst. Solids **40**, 211 (1980).

¹⁹R. A. B. Devine, J. Non-Cryst. Solids **107**, 41 (1988).

²⁰R. T. Williams and E. J. Friebele, in *Handbook of Laser Science and Technology*, edited by M. J. Weber (CRC, Boca Raton, Florida, 1987), Vol. III, Sec. 2.

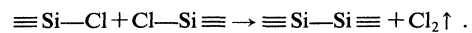
²¹The band position (7.5 eV) and absorption cross section (8×10^{-17} cm²) of Si—Si homobond in ν -SiO₂ is close to those (7.56 eV, 6.0×10^{-17} cm²) of the corresponding absorption band of Si₂H₆ molecule [U. Itoh, Y. Toyoshima, H. Onuki, N. Washio, and T. Ibuki, J. Chem. Phys. **85**, 4867 (1986)].

²²H. Imai, K. Arai, H. Imagawa, H. Hosono, and Y. Abe, Phys. Rev. B **38**, 12 772 (1988).

²³E. P. O'Reilly and J. Robertson, Phys. Rev. B **27**, 3780 (1983).

²⁴The concentrations of oxygen-deficient-type defects are, in general, high in ν -SiO₂ prepared by this process. These de-

fects are considered to be formed via dechlorination process near the surface of the soot particles;



²⁵A. E. Geissberger and F. L. Galeener, Phys. Rev. B **28**, 3266 (1983).

²⁶R. H. Stolen and G. E. Walrafen, J. Chem. Phys. **64**, 2623 (1976).

²⁷W. Primak, E. Edwards, D. Keifer, and H. Szymanski, Phys. Rev. **133**, A531 (1964).

²⁸E. Holzenkampfer, F. W. Richter, J. Stuke, and V. Voegt-Grote, J. Non-Cryst. Solids **32**, 327 (1979).